

# Numerical Simulations of $K_0$ Triaxial Tests on Collapsible Porous Clay

J.C. Ruge<sup>1</sup>, A. López<sup>2</sup>, F.A. Molina-Gómez<sup>3</sup>, R.P da Cunha<sup>4</sup> and J.E. Colmenares<sup>1</sup>

<sup>1</sup>Department of Civil and Agricultural Engineering, Universidad Nacional de Colombia, Bogota, Colombia

<sup>2</sup>Department of Civil Engineering, University Piloto de Colombia, Bogota, Colombia

<sup>3</sup>Department of Engineering, Escuela Militar de Cadetes General "José María Córdova", Bogota, Colombia

<sup>4</sup>Department of Civil and Environmental Engineering, Universidade de Brasília, Brasília, Brazil

E-mail: jcruge@unal.edu.co

**ABSTRACT:** This paper addresses numerical simulations of  $K_0$  triaxial tests performed using a single element program. The methodology was based on construction of numerical models with three different constitutive models in order to represent the soil behaviour during stress path states. The constitutive models used were (i) the Mohr-Coulomb, (ii) the Cam-Clay, and (iii) a hypoplastic model. The material used was a collapsible porous Brazilian clay. The values obtained were compared and calibrated with experimental data. Results show that it is possible to assess soil behaviour via a single element program and that triaxial  $K_0$  stress path tests can be simulated with numerical methods. Results show that it is possible to replicate and calibrate soil behaviour under zero lateral displacement using computational tools.

**Keywords:** Constitutive models,  $K_0$  Triaxial tests, Numerical test simulation, Single element program, Stress path

## 1. INTRODUCTION

Models are useful tools for representing reality (Wood, 2004), and constitutive models can represent soil behaviour mathematically. Nevertheless, the majority of these models assume that the material study is perfectly elastic (Schofield and Wroth, 1968), and many numerical models are designed especially for a specific material. For these reasons, it is common to find models that describe soil behaviour only for particular conditions or specific situations.

Over time, and in various parts of the world, a variety of models have been developed to describe soil responses (Robin *et al.*, 2015). However, many of these models cannot adequately simulate soil responses. The most frequently used are constitutive models for elastoplastic materials. These include the Mohr-Coulomb model and the Cam-Clay model (Ti *et al.*, 2009). On the other hand, Kolymbas (1991) formulated a hypoplastic constitutive model which was originally created for study of granular soils and incorporated the stress-strain rate concept (Lizcano & Kolymbas, 1999). Later, the hypoplastic constitutive model was modified and adapted to clayey soils by Mašin (2005). All of these models can be adjusted and validated via experimental data, as described Lizcano & Kolymbas (2000).

Mendoza & Lizcano (2010) developed an experimental program to compare the behaviour of clayey soils in different constitutive models. They conducted simulations for two soil samples taken from Bogotá, Colombia. The first sample was taken from a site near El Dorado Airport at 3 meters depth. The second sample was taken from the Polo neighbourhood at a depth of 40 m. Later, Mendoza *et al.* (2014) presented an alternative for calibrating constitutive models which is based on the use of a single element program. That work incorporates numerical simulations of the implementation of three constitutive models for structured soils. The study also includes laboratory tests of a porous cemented clay from Brazil.

This paper focuses on evaluation of soil behaviour during  $K_0$  triaxial tests using three different constitutive models. Evaluations were done through numerical simulations in a single element program as proposed by Gudehus *et al.*, (2008). The methodology used to calibrate the parameters of each constitutive model is described later in this study. In addition, this study provides a geotechnical characterization of a collapsible porous clay from Brazil. Finally, a statistical comparison between simulations and laboratory tests is presented.

## 2. BACKGROUND FOR CONSTITUTIVE MODELS

For Kolymbas (2000), a constitutive model is a mathematical formulation capable of describing the microscopic physical

performance of an ideal soil. The aim of a constitutive model is to establish a soil's stress-strain behaviour based on theories of elasticity, plasticity, viscoplasticity, micro-fracturing and damage mechanics either combined or separately (Desai, 2005). Consequently, the formulation only represents a simplified hypothesis of conditioned reality. Hence, each constitutive model must be used for the parameters and materials for which it was developed (González-Cueto *et al.*, 2013).

### 2.1 Mohr-Coulomb model

The Mohr-Coulomb model is widely used in geotechnical engineering to determinate shear strength even though the model does not consider effects under different stress paths. Camacho-Tauta *et al.* (2015) write that the Mohr-Coulomb model is an elastic plastic-perfect model which was developed from Hooke's law of elasticity. In contrast, Nieto Leal *et al.* (2009) say that the model includes a unique and fixed yield surface associated with irreversible plastic deformations. This yield criterion is an extension of Coulomb's law of friction for a specific stress state. Equation 1 presents the constitutive law for the Mohr-Coulomb model.

$$f = \frac{1}{2}(\sigma_1 + \sigma_3) \sin \varphi - \frac{1}{2}(\sigma_1 - \sigma_3) - c \cos \varphi \quad (1)$$

Perfect elastoplastic behaviour in the model is formulated from the relationship between elastic and plastic deformations by applying Hooke's law in its classic form (Nieto Leal, Camacho-Tauta and Ruiz Blanco, 2009) as presented in Equation 2.

$$\dot{\sigma} = D^e \dot{\varepsilon}^e = D^e \dot{\varepsilon}^e = D^e (\dot{\varepsilon} - \dot{\varepsilon}^p) \quad (2)$$

The model also includes a flow rule. This rule presents a function for plastic potential ( $g$ ) which is accompanied by a yield point ( $f$ ). According to the plasticity law, a condition of the Mohr-Coulomb is that  $g \neq f$ . Therefore, the plastic potential is described by equation 3.

$$g = \frac{1}{2}(\sigma_1 + \sigma_3) - \frac{1}{2}(\sigma_1 - \sigma_3) \sin \psi \quad (3)$$

Given the flow rule, the model has five (5) input parameters (Camacho-Tauta, Molina-Gómez and Reyes-Ortiz, 2015): Young's Modulus ( $E$ ) is the ratio of the increased stress and the corresponding strain change; Poisson's ratio ( $\nu$ ) is the relationship between transverse and longitudinal deformation; cohesion ( $c$ ) is the attraction and intermolecular forces between soil particles and water films; the friction angle ( $\varphi$ ) is the angle generated by the particles in

a material at rest; and the dilatancy angle ( $\psi$ ) indicates the increasing volume of a granular material due to shear stresses.

### 2.2 Cam-Clay model

The Cam-Clay is an elasto-plastic model for describing the behaviour of clayey soil (Camacho-Tauta, Reyes-Ortiz and Bueno Pumarejo, 2004). According to Wood (1991), this constitutive model permits simulation of the stress-strain relationship in triaxial tests. The model was formulated by researchers at Cambridge University during the 1960s (Atkinson, 2007), but the Cam-Clay model establishes that the soil has a yield surface and an associative flow rule. Equation 4 describes the principle of its formulation.

$$\frac{p'}{p'_o} = \frac{M^2}{M^2 + \eta^2} \quad (4)$$

The yield surface represents the various combinations of stresses that cause permanent deformations while the yield surface symbolizes a geometrical place in a  $p$ - $q$  plane which delimits the elastic strains. Experimental evidence indicates that an elliptical yield surface is a reasonable approximation for soils (Wong and Mitchell, 1975). The higher the preconsolidation stress, the larger the initial ellipse. Figure 1 shows a representation of the model.

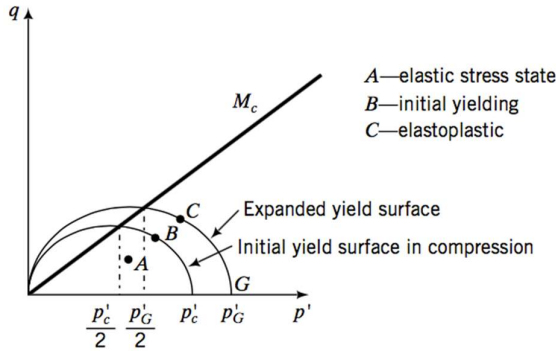


Figure 1 Yield surface of Cam-Clay model (Budhu, 2010)

The constitutive formulation includes five different parameters  $\lambda$ ,  $\kappa$ ,  $M$ ,  $E$  and  $\nu$  where  $\lambda$  is the slope of the loading branch,  $\kappa$  is the slope of the unloading branch,  $M$  is the slope of the critical state,  $E$  is the elastic modulus, and  $\nu$  is Poisson's ratio.

### 2.3 Hypoplastic model

The hypoplastic model represents non-linear soil behaviour. It was initially formulated by Kolymbas (1985) for sandy soils but was later adapted by Mašin (2005) to simulate behaviour of clayey soils. Equation 5 shows this model's initial stress tensor for evaluating soil dependency of stress level and density.

$$T = f_s(L: D + f_d N \parallel D \parallel) \quad (5)$$

where  $f_s$  and  $f_d$  incorporate the effect of barotropy and pyknotropy of soil,  $L$  and  $N$  are the constitutive tensors of third and fourth order, respectively, and  $D$  is Euler's elongation tensor. Equations 6-9 express the mathematical sense of all of the above parameters.

$$L = \frac{1}{\bar{T} \cdot \bar{T}} (C_1 F^2 I + C_2 a^2 \bar{T} \otimes \bar{T}) \quad (6)$$

$$N = L: -Y \left( \frac{m}{\parallel m \parallel} \right) \quad (7)$$

$$f_s = - \frac{tr T}{\lambda_*} (3 + a^2 - 2^a a \sqrt{3})^{-1} \quad (8)$$

$$f_d = - \left[ \frac{2tr T}{3pr} e^{\left( \frac{\ln(1+e)-N}{\lambda} \right)} \right]^\alpha \quad (9)$$

Like the Cam-Clay model, this constitutive model requires five parameters (Ruge, da Cunha and Rondón, 2014):  $\lambda$  and  $\kappa$  are computed from the slope of the loading and unloading branches of a consolidation test;  $N$  is the second-order tensor model obtained from the consolidation graph by calculating the point where the graph crosses the ordinate axis,  $r$  is the ratio of the bulk modulus and the undrained shear modulus, and  $\varphi_c$  can be calculated by linear regression from an MIT-type stress state graph.

## 3. METHODOLOGY

### 3.1 Materials

Samples of collapsible porous clay from Brazil were used in this study. The specimens were extracted from the federal district of Brasilia at a depth of 11 meters. According to Ruge (2014), the soil of Brasilia is composed of red clay with a high void ratio and low specific weight. This soil is usually red due to the presence of iron. In addition, soils in the city of Brasilia city are highly weathered and leached due to the soil formation process. Figure 2 shows typical stratification of this zone obtained from SPT and CPT tests.

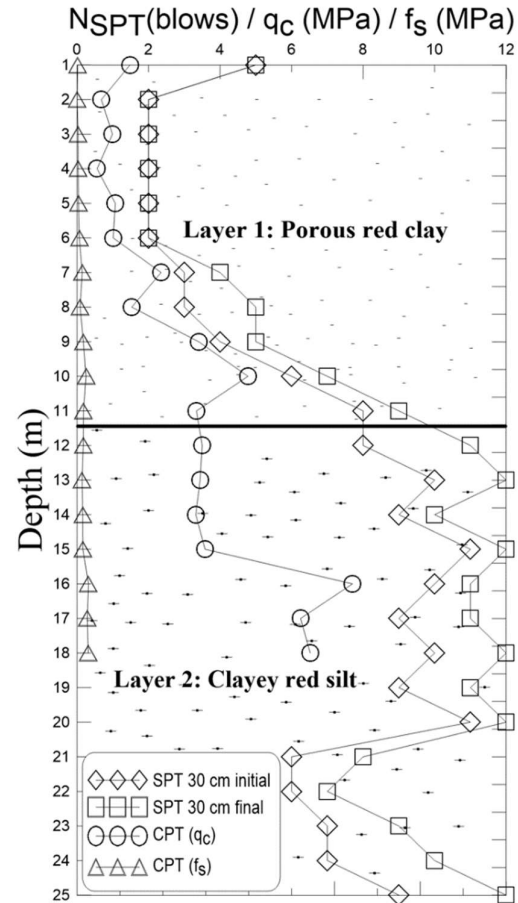


Figure 2 Typical stratigraphic profile

### 3.2 Experimental program

Three different samples were subjected to an experimental program that included physical and mechanical laboratory tests. Table 1 shows their physical properties, and Figure 3 shows grain size distributions of all three samples.

Table 1 Physical properties of soils.

Sample	Depth (m)	Gs	LL (%)	LP (%)	IP (%)	$\omega_0$ (%)
1	3.00-3.25	2.65	56.4	31.2	25.2	35
2	6.00-6.30	2.66	59.8	34.6	25.2	32
3	8.70-9.00	2.63	66.8	36.4	30.4	30

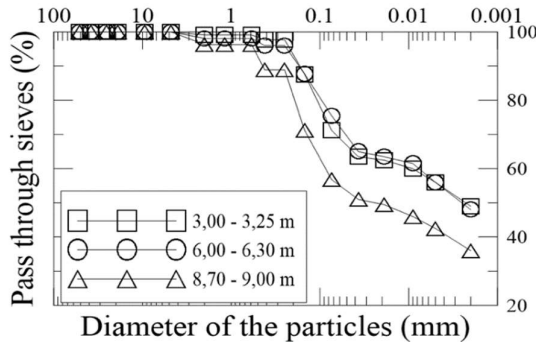


Figure 3 Grain size distribution

A porosimetry test which measures pore size and distribution of a soil sample was used to establish whether the materials tested were porous clay. Apparent density can also be calculated from these test results. The test process consists of mercury intrusion to estimate capillary pressures inside of soil voids. Once plotted, inflexion points represent the presence of micro and macro pores. Figure 4 shows pore size distribution (PSD).

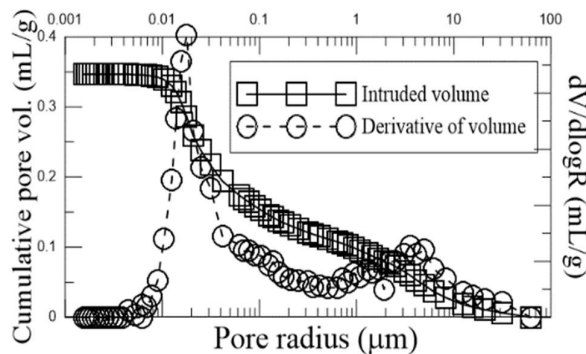


Figure 4 PSD of the Brazilian clay

Micro-structural photographs taken by a Scanning Electronic Microscope (SEM) confirmed porosimetry test results. Figure 5 shows a site where it is possible to observe the size of the micropores in one sample at close to nano scale.

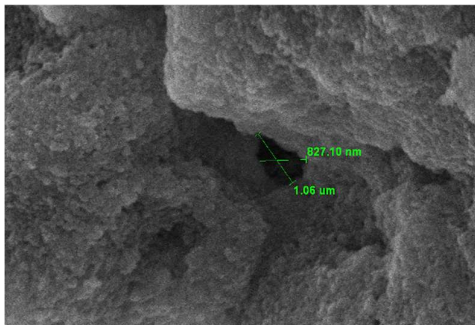


Figure 5 SEM Image of the soil under study

### 3.3 $K_0$ triaxial tests

The mechanical behaviour of different geotechnical structures is controlled by the coefficient of earth pressure at rest  $K_0$ . For normally consolidated clays the best accepted model is that proposed by Jaky (1944) which is presented in equation 10. Nevertheless, there is still no methodology for determining the initial stress state in geotechnical problems that include overconsolidated clays (Boháč *et al.*, 2013).

$$K_0 = 1 - \sin \phi \tag{10}$$

The procedure used to consolidate a soil at rest in the  $K_0$  condition without lateral strain consists of applying small loading steps of confining pressure combined with interrupted imposition of axial load. In this type of triaxial test, the confining pressure is varied in order to keep radial deformation at zero as the vertical stress increases (Campanella & Vaid, 1972). For this reason, the equipment must be instrumented with local sensors to evaluate soil behaviour under anisotropic conditions (Molina-Gómez, Camacho-Tauta and Reyes-Ortiz, 2016). Figure 6 shows the boundary conditions and path stress characteristics of the  $K_0$  triaxial test.

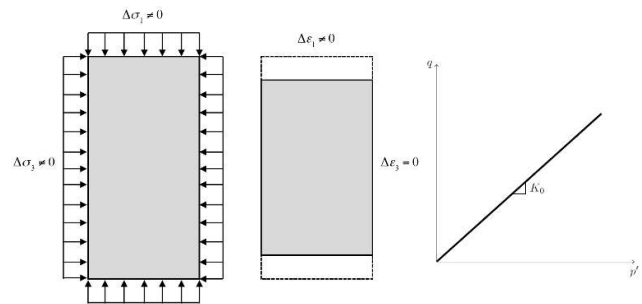


Figure 6 Boundary conditions and stress paths in  $K_0$  triaxial test

A GDS True Triaxial Apparatus (GDSTTA) was used for performance of stress paths (Figure 7). This apparatus allows a wider range of complex stress paths to be performed since it has one vertical and one horizontal dynamic load actuator (axis 1 and 2). Stress control is provided for the second horizontal axis (axis 3) via cell pressure (GDS, 2017). The device was equipped with two electro-mechanical load actuators of 10 kN and one proximator. In addition, vertical load on axis 1 and 2 was controlled by the actuators while it was controlled by lateral displacement on axis 3.

Nine different cuboidal soil samples of 75 mm x 75 mm x 150 mm were tested to estimate  $K_0$  value under conditions of natural and saturated water contents. Tests of two specimens of each sample were performed under natural water content conditions to guarantee greater reliability for the  $K_0$  values obtained. These tests were performed without suction control in the samples. Tests under saturated conditions were performed on a single specimen. In addition, these samples were saturated by water percolation and backpressure application until they reach a Skempton's B-value higher than 0.95.

Drainage was allowed under both water conditions. Outcomes obtained in the laboratory tests were plotted on a graph that correlated axial stresses with confining stresses ( $\sigma_1$  vs  $\sigma_3$ ). According to (Fahey, 1992), the slope of the line obtained corresponds to the  $K_0$  value (see equation 11). For this reason, this paper does not use the  $p$ - $q$  diagram to represent the stress path during numerical simulations.

$$K_0 = \frac{\sigma_3}{\sigma_1} \tag{11}$$

Figure 8 presents the test results for evaluation of  $K_0$  and triaxial test results are presented in Table 2. The values of  $K_0$  indicated in the table were obtained through linear regression.

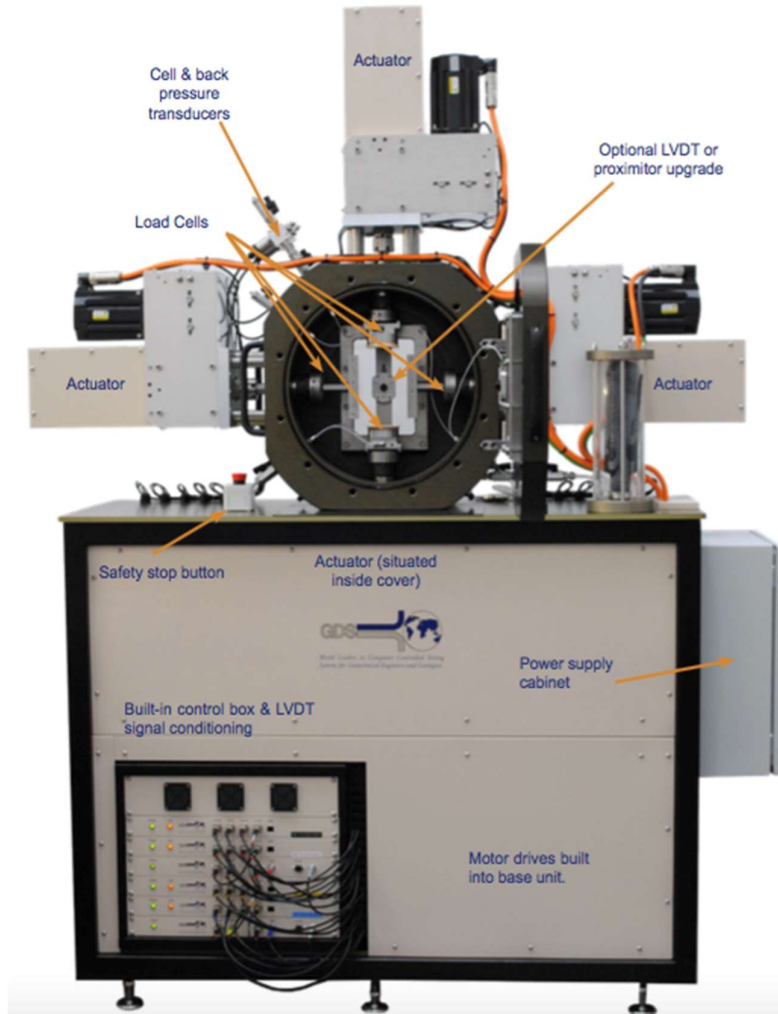


Figure 7 GDSTTA (GDS, 2017)

Table 2 Summary of  $K_0$  triaxial compression testing

Sample/Depth (m)	Spec	Initial conditions	$K_0$
1 3.00 - 3.30	1- $h_{nat}$	$h_{nat}=34.10\%/e=1.575/S=58.4\%$	0.44
	2- $h_{nat}$	$h_{nat}=33.51\%/e=1.633/S=55.4\%$	0.44
	3-Sat	$h_{nat}=33.80\%/e=1.633/S=60.7\%$	0.43
2 6.00 - 6.30	1- $h_{nat}$	$h_{nat}=31.90\%/e=1.234/S=70.1\%$	0.50
	2- $h_{nat}$	$h_{nat}=32.00\%/e=1.178/S=73.6\%$	0.50
	3-Sat	$h_{nat}=32.40\%/e=1.310/S=67.0\%$	0.46
3 8.70 - 9.00	1- $h_{nat}$	$h_{nat}=30.10\%/e=1.125/S=71.9\%$	0.54
	2- $h_{nat}$	$h_{nat}=29.70\%/e=1.117/S=71.4\%$	0.53
	3-Sat	$h_{nat}=29.60\%/e=1.103/S=72.1\%$	0.53

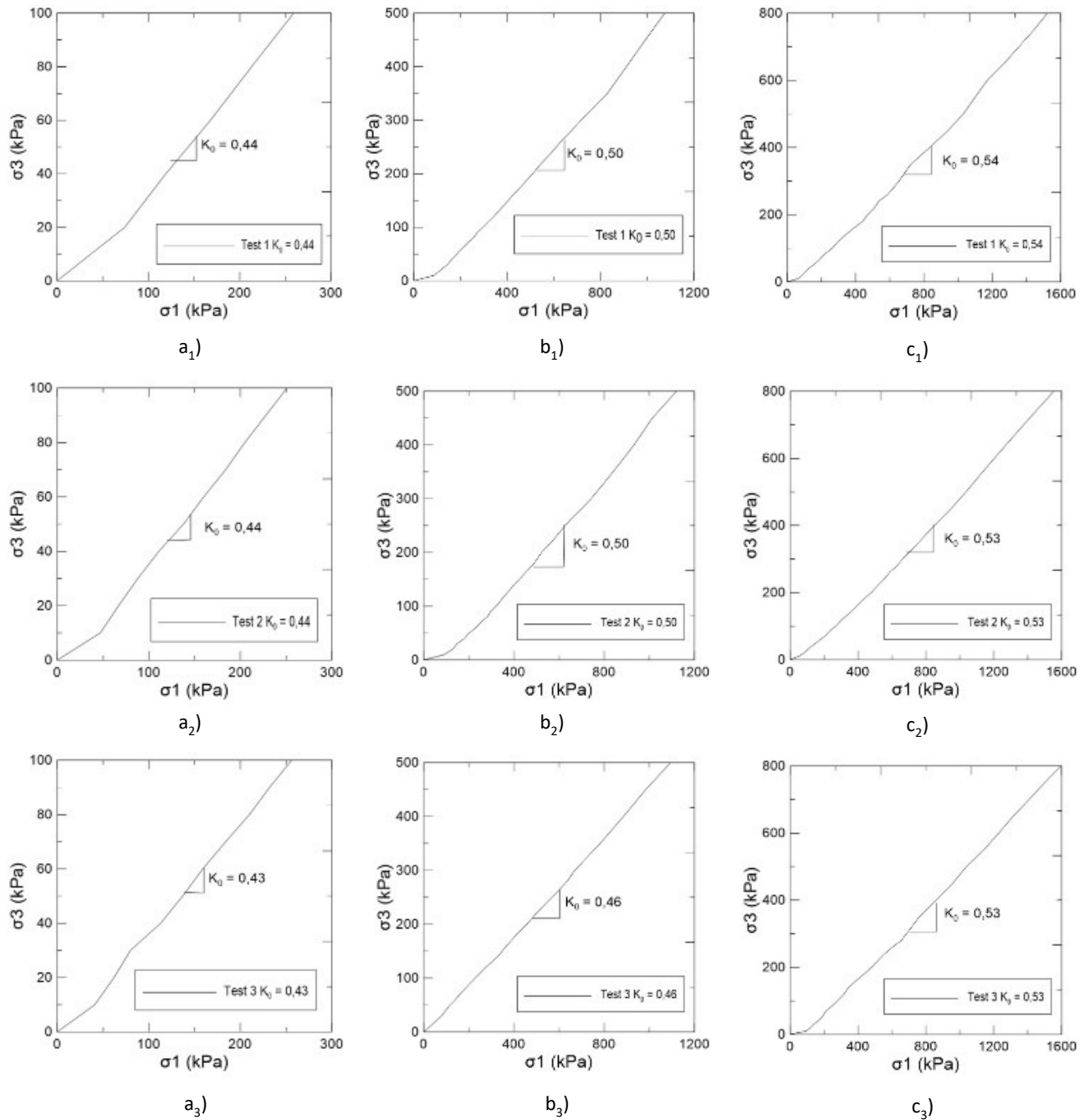


Figure 8 Triaxial  $K_0$  results for Sample 1, Sample 2 and Sample 3. a) natural water content, b) natural water content, c) saturated

## 4. RESULTS AND ANALYSIS

### 4.1 Calibration of parameters

Three constitutive models were used for numerical simulations of the  $K_0$  stress path in triaxial tests, but performance of computational tests required prior calibration of all parameters in each model. Afterwards, the three constitutive models were evaluated to determine which best replicated soil behaviour according to the experimental data. The methodology for calibrating the parameters of the three constitutive models is presented below.

#### 4.1.1 Calibration of the Mohr-Coulomb constitutive model

In engineering practice, the Mohr-Coulomb model is the most frequently used. Its parameters represent real mechanical properties of the soil, and its main characteristic is that strength is dependent on confining stress. Calibration of the five parameters ( $\phi$ ,  $E$ ,  $\nu$ ,  $\psi$  and  $c$ ) of the Mohr-Coulomb model is relatively simple, but stress level to which the soil is subjected and other issues must be considered. Peak deviator stress ( $q$ ) is very useful because, among other reasons, 50% of  $q$  can be used to estimate the secant modulus and to select Young's Modulus  $E$ . Cohesion ( $c$ ) and the friction angle ( $\phi$ ) were calibrated from of the peak state according to the procedure of Suchomel & Mašin (2009). Figure 9 shows this calibration methodology.

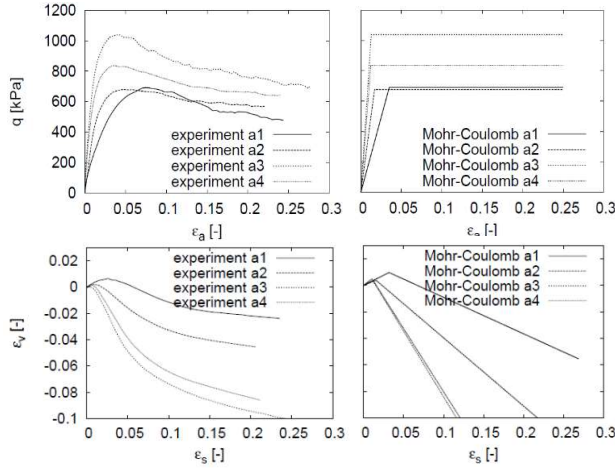


Figure 9 Typical calibration of the Mohr-Coulomb model through comparison of test and predictions. Modified from Suchomel & Mašín (2010)

Poisson’s ratio ( $\nu$ ) can be defined in accordance with the drainage condition of the test or even of the geotechnical problem addressed. In some cases, such as sandy soils and overconsolidated clays it is possible to find it by using the contractive part in the  $\Delta\epsilon_v$  vs.  $\Delta\epsilon_s$  space by means of equation 8. Similarly, dilatancy can be calculated from equation 9 (see Figure 5). Table 3 shows calibration of the Mohr-Coulomb model with these methods.

$$\nu = \frac{\Delta\epsilon_a - \Delta\epsilon_v}{2\Delta\epsilon_a} \tag{12}$$

$$\frac{\Delta\epsilon_v}{\Delta\epsilon_s} = \frac{6\sin\psi}{3\sin\psi} \tag{13}$$

Table 3 Calibration of the Mohr-Coulomb model.

$E$ (kPa)	$\nu$ (-)	$c$ (kPa)	$\phi$ (°)
11500	0.32	11	32

4.1.2 Calibration of the Cam Clay constitutive model

Determination of Cam Clay model parameters requires an elastic and plastic characterization to evaluate the mechanical behaviour of the soil. To analyse elastic response, the shear modulus  $G$  and strain modulus  $K$  must be obtained following Equations 14 and 15 (see Figure 10). Consequently, it is necessary to perform various conventional triaxial tests from which the elastic parameters and some of the plastic parameters of the model can be obtained.

$$K = \frac{E}{3(1-2\nu)} \tag{14}$$

$$G = \frac{3(1-2\nu)}{2(1+\nu)} \tag{15}$$

The plastic response can be obtained by using  $M$  and  $\lambda$ . Thus, it is necessary to obtain these parameters simultaneously through oedometric and triaxial tests. Figure 11 graphically presents the procedure for capturing model parameters and comparing the constitutive equations with the tests results. Table 4 summarizes calibration results.

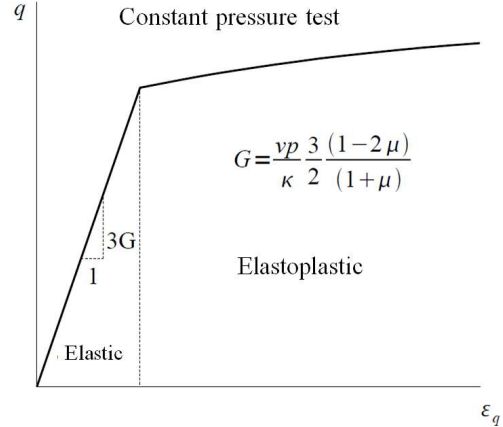


Figure 10 Graphic representation of the shear modulus  $G$

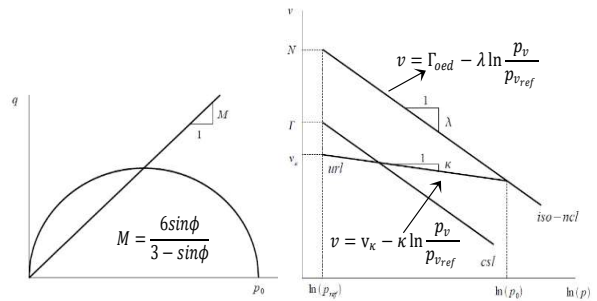


Figure 11 Graphic representation of  $M$ ,  $\lambda$ ,  $\kappa$  and  $\Gamma$

Table 4 Calibration of the Cam-Clay model

$E$ (kPa)	$\nu$ (-)	$M$ (-)	$\lambda$ (-)	$\kappa$ (-)
11500	0.32	1.18	0.0696	0.0057

5.1.3 Calibration of the Hypoplastic constitutive model

Simulation of the oedometric test was used to calibrate  $N$ ,  $\lambda$  and  $\kappa$  as shown in Figure 12.

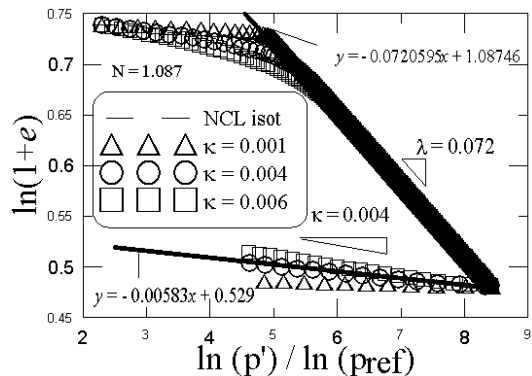


Figure 12 Calibration of  $N$ ,  $\lambda$  and  $\kappa$  (Ruge, 2014)

This test evaluated the behaviour of the State Boundary Surface (SBS) whose shape depends on the model parameter, especially on  $\lambda$ ,  $\kappa$  and  $\phi_c$  (Ruge et al., 2013). These parameters were calibrated based on isotropic tests of loading and unloading (Figure 9, left).  $\lambda$  was obtained from the normal consolidation line (NCL) since this corresponds to its slope.  $\kappa$  was calibrated by the slope of the isotropic unloading section close to the normally consolidated state. It is important to note that the model selected predicts the isotropic unloading line in the  $e$  vs  $\ln p'$  space with a value exactly equal to  $\kappa$  during unloading of the normally consolidated state. In addition, it is clear that all admissible states of a soil are inside of a surface in the stress-void ratio space. This surface corresponds to the SBS and is a surface in 3D space.

On the other hand,  $r$  can be defined directly like the relationship between the bulk volumetric modulus and the shear modulus which were obtained from numerical tests that start with an isotropic, normally consolidated, stress state. However, since the model predicts a gradual degradation of shear stiffness, it is advisable to find an appropriate value for  $r$  through a parametric study (Ruge, 2014). This approach is valid because interrelations with other parameters of the model do not exist (Masin & Herle, 2005).

The critical friction angle  $\phi_c$  is a soil parameter which is measured once it reaches a state. Its volume does not change during the process of deformation or loading. Hence,  $\phi_c$  is a relationship of the principal stresses at the critical state, and it is the theoretical basis of most modern constitutive models since it defines the critical state of each material. In this phase, the material presents infinite strains at constant stress and volume regardless of the stress level. Linear regression using the critical state points of the triaxial tests is necessary for finding  $\phi_c$ . Table 5 shows the parameters calibrated for the Hypoplastic model.

Table 5 Calibration of the Hypoplastic model

$\lambda$	$\kappa$	$N$	$r$	$\phi_c$
(-)	(-)	(-)	(-)	(°)
0.0696	0.0057	34.6	0.10	35

4.2 Numerical simulations

The single element program is a useful tool for computer simulation of laboratory tests. This kind of program provides a choice of the type of experiment, the load application, and/or the speed of deformation. In addition, it can replicate drained or undrained triaxial tests. One of the most common Single Element Programs is *Incremental Driver*. Created by Niemunis (2007), its code was formulated in Fortran, and it is free access software. Moreover, *Incremental Driver* can evaluate soil behaviour by applying different constitutive models.

The in-situ stress state is very difficult to obtain although the value of  $K_0$  can be determined by using either laboratory or field tests. Generally, in-situ tests are more reliable because they can be performed under conditions close to natural conditions at a given depth. This is especially true for the self-boring pressuremeter (Lo & Chu, 1991). Nevertheless, it is possible to identify proximity of numerical simulations to in-situ conditions as reported by Huat et al. (2012). For this reason, numerical simulations could be used to obtain results which approximate those under real conditions of the collapsible porous clay from Brazil.

Numerical simulations, using the three constitutive models, were performed. Figure 13 displays the results of nine different experiments based on a single element program. These numerical simulation results were compared to the results from all of the samples tested, and an analysis of variance (ANOVA) was conducted (see Table 6) in order to compare variation between the numerical simulation results and laboratory results.

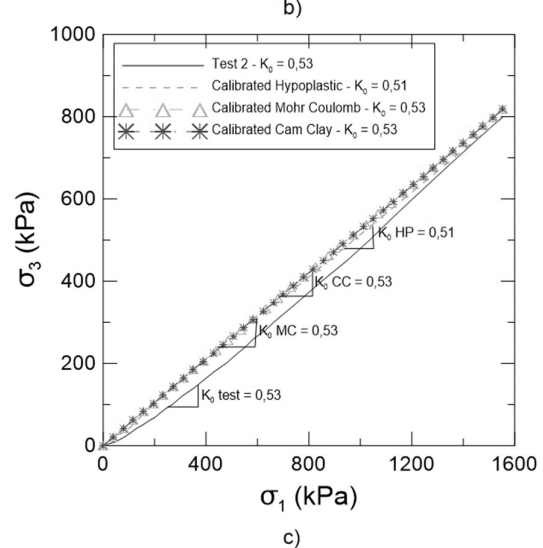
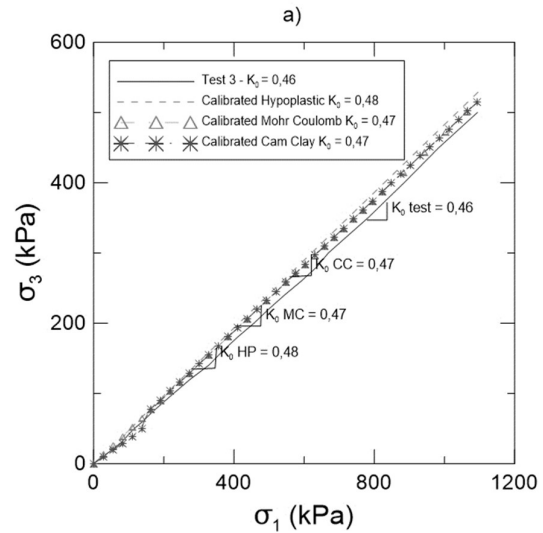
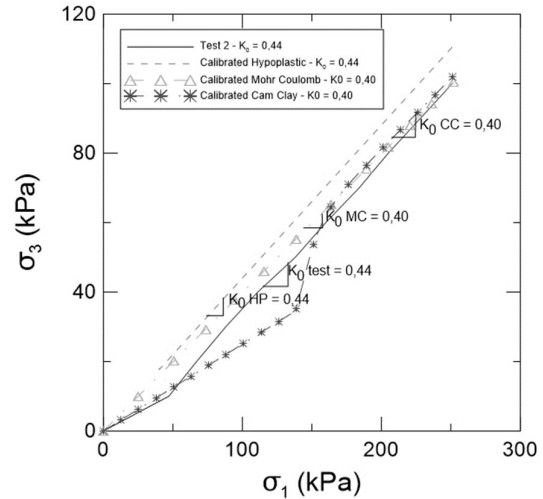


Figure 13 Numerical simulation results. a) Sample 1, b) Sample 2., c) Sample 3

Table 6 ANOVA results

Source	Degrees of freedom	Sum of squares	Mean sum of squares	F-test	p-value
$K_0$ of the model	3	0.0003	0.0001	0.0340	0.9908
Residuals	8	0.0239	0.0030		

ANOVA shows that numerical simulations results and laboratory values are statically equal at a 99% confidence level ( $\alpha=0.01$ ). This is due to the fact that in  $K_0$  paths the soil does not reach failure and therefore does not have plastic deformations. Apparently, all models adequately reproduce soil responses for isotropic conditions. Nevertheless, However, Tukey’s method Tukey (1949) was used to calculate multiple comparisons. Tukey’s method is based on the assumption that the confidence intervals of the means (1-  $\alpha$ ) contain their corresponding mean difference in each modelling of the laboratory results. Figure 14 shows multiple comparison results and presents the relationships among all the results. This graph groups data around a common point, which in this case is 0. The results indicate that the model with the best correspondence with the laboratory values is the hypoplastic model.

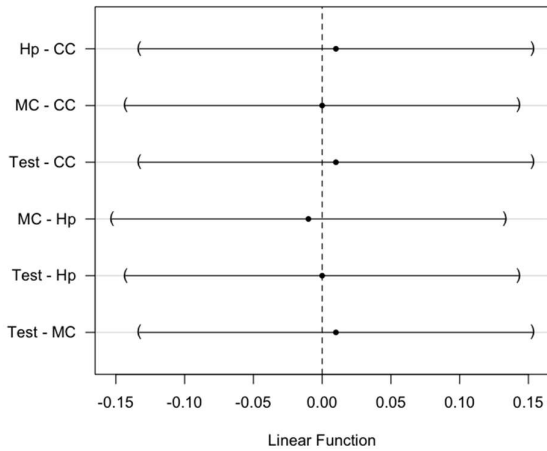


Figure 14 Multiple comparison by Tukey’s method

5. CONCLUSIONS

This study proposes an alternative methodology for modelling the  $K_0$  value of collapsible porous clay from Brazil. The method is based on using numerical simulations to replicate laboratory isotropic compression tests. The technique has been proven to work with different constitutive models.

Although the single element program is a useful tool, the critical stage of parameter calibration is exhaustive work that cannot usually be avoided because there are so few references related to this type of work. In addition, preliminary information about the soil behaviour is necessary for establishing whether the outcomes of the program make physical sense and represent the soil’s response.

For the soil studied, it was found that all models reproduce properly the  $K_0$  path. Moreover, a statistical assessment revealed that the hypoplastic model is the best fit for the experimental data. Nevertheless, all of the constitutive models replicated soil behaviour and any one of them can be used to find  $K_0$  through a single element program.

The numerical simulations to obtain  $K_0$  can be used as an alternative in geotechnical engineering. Since the initial conditions are difficult to simulate because they depend on the history of stress of the soil, it is important to use this before starting rather than after the final procedure of the simulation.

6. NOTATION

- $D$  : Euler’s elongation tensor
- $D^e$  : Stiffness matrix (elastic)
- $E$  : Young’s modulus
- $f$  : Yield point
- $f$  : Pyknotropy effect
- $f$  : Yield point
- $K_0$  : Coefficient of earth pressure at rest
- $g$  : Plastic potential
- $G$  : Shear modulus
- $K$  : Bulk modulus
- $M$  : Slope of critical state line
- $N$  : Constitutive tensor of fourth order
- $p'$  : Effective mean stress
- $p'_0$  : Equivalent consolidation pressure
- $q$  : Deviator stress
- $r$  : Moduli ratio ( $K/G$ )
- $\mathcal{L}$  : Constitutive tensor of third order
- $\alpha$  : Significance level
- $\Delta\varepsilon_v$  : Vertical strain change
- $\Delta\varepsilon_r$  : Radial strain change
- $\dot{\varepsilon}^e$  : Elastic strain
- $\dot{\varepsilon}^p$  : Plastic strain
- $\eta$  : Stress ratio ( $p'/q$ )
- $\kappa$  : Slope of unload-reload line
- $\lambda$  : Slope of normal consolidation line
- $\varphi$  : Friction angle
- $\varphi_c$  : Friction angle at the critical state
- $\psi$  : Dilatancy angle
- $\dot{\sigma}$  : Normal stress
- $\sigma_1$  : Major principal stress
- $\sigma_3$  : Minor principal stress
- $\nu$  : Poisson’s ratio

7. REFERENCES

Atkinson, J. (2007) The Mechanics of Soils and Foundations. 2nd ed. CRC Press Book.

Boháč, J. et al. (2013) ‘Methods of determination of  $K_0$  in overconsolidated clay’, in Delage, P. et al. (eds) Proceedings of the 18th International Conference ICSMGE. Paris, pp. 203–206.

Budhu, M. (2010) Soil Mechanics and Foundations. 3rd ed. New York: Wiley.

Camacho-Tauta, J. F., Molina-Gómez, F. A. and Reyes-Ortiz, O. (2015) ‘Simulation of traffic loading on an embankment by the finite element method with different soil models’, in Rinaldi, V. A. (ed.) Six International Symposium on Deformation Characteristics of Geomaterials. Buenos Aires, pp. 737–744. doi: 10.3233/978-1-61499-601-9-737.

Camacho-Tauta, J. F., Reyes-Ortiz, Ó. J. and Bueno Pumarejo, P. B. (2004) ‘Utilización del modelo Cam-Clay modificado en suelos cohesivos de la sabana de Bogotá’, Ciencia e Ingeniería Neogranadina. Universidad Militar Nueva Granada, (14), pp. 1–13.

Desai, C. S. (2005) ‘Constitutive Modeling for Geologic Materials: Significance and Directions’, International Journal of Geomechanics. American Society of Civil Engineers, 5(2), pp. 81–84. doi: 10.1061/(ASCE)1532-3641(2005)5:2(81).

Fahey, M. (1992) ‘Measuring  $K_0$  in the triaxial test’, Australian Geomechanics Journal, 26, pp. 620–62.

GDS (2017) GDS True Triaxial Apparatus. Available at: <http://www.gdsinstruments.com/gds-products/gds-true-triaxial-apparatus> (Accessed: 2 August 2017).

González-Cueto, O. et al. (2013) ‘Análisis de los modelos constitutivos empleados para simular la compactación del suelo mediante el método de elementos finitos’, Revista



- Ciencias Técnicas Agropecuarias. Universidad Agraria de La Habana, 22(3), pp. 75–80.
- Gudehus, G. et al. (2008) ‘The soilmodels.info project’, *International Journal for Numerical and Analytical Methods in Geomechanics*. John Wiley & Sons, Ltd., 32(12), pp. 1571–1572. doi: 10.1002/nag.675.
- Huat, B. B. K., Prasad, A. and Toll, D. G. (2012) *Handbook of tropical residual soils engineering*. 1st ed. CRC Press/Balkema.
- Jaky, J. (1944) ‘The coefficient of earth pressure at rest. In Hungarian “A nyugalmi nyomás tenyezője”’, *Journal Society Hungarian Engineering and Architecture*, pp. 355–358.
- Kolymbas, D. (1985) ‘A generalized hypoplastic constitutive law’, in 11th International Conference SMFE. San Francisco: Balkema, p. 2626.
- Kolymbas, D. (1991) ‘An outline of hypoplasticity’, *Archive of Applied Mechanics*, 61(3), pp. 143–151. doi: 10.1007/BF00788048.
- Kolymbas, D. (Dimitrios) (2000) *Introduction to hypoplasticity*. 1st ed. A.A. Balkema.
- Lizcano, A. and Kolymbas, D. (1999) ‘Hipoplasticidad Contra Elastoplasticidad (Parte I)’, *Revista de Ingeniería*, 10(11), pp. 25–31. doi: 10.16924/riua.v0i11.577.
- Lizcano, A. and Kolymbas, D. (2000) ‘Hipoplasticidad Contra Elastoplasticidad (Parte II)’, *Revista de Ingeniería*, 11(10), pp. 59–69. doi: 10.16924/riua.v0i10.583.
- Mašín, D. (2005) ‘A hypoplastic constitutive model for clays’, *International Journal for Numerical and Analytical Methods in Geomechanics*, 29(4), pp. 311–336. doi: 10.1002/nag.416.
- Mendoza, C., Farias, M. and da Cunha, R. P. (2014) ‘Validación de modelos constitutivos avanzados de comportamiento mecánico para la arcilla estructurada de Brasilia’, *Obras y proyectos*. Universidad Católica de la Santísima Concepción, (15), pp. 52–70. doi: 10.4067/S0718-28132014000100005.
- Mendoza, C. and Lizcano, A. (2010) ‘Comportamiento Anisotrópico de la Arcilla de Bogotá’, in XIII CONGRESO COLOMBIANO DE GEOTECNIA. Manizales: Universidad Nacional de Colombia.
- Molina-Gómez, F. A., Camacho-Tauta, J. F. and Reyes-Ortiz, O. J. (2016) ‘Stiffness of a granular base under optimum and saturated water contents’, *Revista Tecnura*, 20(49), pp. 75–85. doi: dx.doi.org/10.14483/udistrital.jour.tecnura.2016.3.a05.
- Niemunis, A. (2007) *Incremental Driver - User Manual*. 1st ed.
- Nieto Leal, A. E., Camacho-Tauta, J. F. and Ruiz Blanco, E. F. (2009) ‘Determinación de parámetros para los modelos elastoplásticos Mohr-Coulomb y Hardening Soil en suelos arcillosos’, *Revista Ingenierías Universidad de Medellín*, 8(15), pp. 75–91.
- Robin, V. et al. (2015) ‘An effective constitutive model for lime treated soils’, *Computers and Geotechnics*, 66, pp. 189–202. doi: 10.1016/j.compgeo.2015.01.010.
- Ruge, J. C. (2014) *Análise do comportamento de cortina de estacas executada em solo poroso metaestável mediante o uso de um modelo constitutivo hipoplástico considerando a resposta não saturada*. Universidade de Brasília.
- Ruge, J. C., Da Cunha, R. P. and Rondón, H. (2014) ‘Simulación de pruebas de carga en pilotes usando un modelo constitutivo hipoplástico’, *Revista EIA*, 11(21), pp. 171–183.
- Schofield, A. N. and Wroth, C. P. (1968) *Critical State Soil Mechanics*. doi: 10.1111/j.1475-2743.1987.tb00718.x.
- Suchomel, R. and Mašín, D. (2010) ‘Spatial variability of soil parameters in an analysis of a strip footing using hypoplastic model’, in Benz, T. and Steinar, N. (eds) *Numerical Methods in Geotechnical Engineering*. 7th ed. NORWAY: CRC Press/Balkema, pp. 383–388.
- Ti, K. S. et al. (2009) ‘A Review of Basic Soil Constitutive Models for Geotechnical Application’, *EJGE*, 14(J), p. 18.
- Tukey, J. W. (1949) ‘Comparing Individual Means in the Analysis of Variance’, *Biometrics*. International Biometric Society, 5(2), p. 99. doi: 10.2307/3001913.
- Wong, P. K. and Mitchell, R. J. (1975) ‘Yielding and plastic flow of sensitive cemented clay’, *Géotechnique*. Thomas Telford Ltd, 25(4), pp. 763–782. doi: 10.1680/geot.1975.25.4.763.
- Wood, D. M. (1991) *Soil Behaviour and Critical State Soil Mechanics*. 1st ed. Cambridge University Press.
- Wood, D. M. (2004) *Geotechnical Modelling*. 1st ed. Milton Park, Abingdon: CRC Press.